Synthesis and Structural Characterisation† of Some Tetrahedral Platinum–Gold Cluster Compounds containing the Sulphur Dioxide Ligand

D. Michael P. Mingos * and Robert W. M. Wardle
Inorganic Chemistry Laboratory, University of Oxford, South Parks Road, Oxford OX1 3QR

The compound $[Pt_3Au(\mu\text{-}CO)_3\{P(C_6H_{11})_3\}_4]PF_6$ has been synthesised from $[Pt_3(\mu\text{-}CO)_3\{P(C_6H_{11})_3\}_3]$ and $[AuCl\{P(C_6H_{11})_3\}]$ in the presence of $TlPF_6$. It reacts with SO_2 to give a tetrahedral platinum–gold cluster compound $[Pt_3Au(\mu\text{-}CO)_2(\mu\text{-}SO_2)\{P(C_6H_{11})_3\}_4]PF_6$ (**1**) in which one of the CO ligands of the starting material has been replaced by SO_2. Compound (**1**) crystallises in the orthorhombic space group $Pn2_1a$ with four formula units in a cell of dimensions a = 18.671(4), b = 19.618(3), and c = 28.162(4) Å. The compound $[Pt_3(\mu\text{-}SO_2)_3\{P(C_6H_{11})_3\}_3]$ reacts with $[AuCl\{P(C_6H_4F\text{-}p)_3\}]$ to give the tetrahedral platinum–gold cluster compound $[Pt_3Au(\mu\text{-}SO_2)_2(\mu\text{-}Cl)\{P(C_6H_{11})_3\}_3\{P(C_6H_4F\text{-}p)_3\}]$ (**2**) in which one of the SO_2 ligands of the starting *triangulo*-cluster has been replaced by a bridging chloride. Compound (**2**) crystallises in the monoclinic space group $P2_1/n$ with four formula units in a cell of dimensions a =25.490(4), b = 25.855(6), c = 13.819(4) Å, and β = 96.98(2)°. The bonded bridging ligand atoms are approximately coplanar with the metal triangles whilst the metal–phosphine bonds point towards the centre of the metal tetrahedron. N.m.r. studies, $^{31}P\text{-}\{^1H\}$ and $^{195}Pt\text{-}\{^1H\}$, suggest that the solid-state structures are retained in solution for both compounds. The reaction of $[Pt_3(\mu\text{-}SO_2)_3\{P(C_6H_{11})_3\}_3]$ with $[AuCl\{P(C_6H_{11})_3\}]$ in the presence of $TlPF_6$ gives $[Pt_3Au(\mu\text{-}SO_2)_3\{P(C_6H_{11})_3\}_4]PF_6$ which may be converted into (**1**) by reaction with CO. The compound $[Pt_3(\mu\text{-}SO_2)_3\{P(C_6H_{11})_3\}_3]$ reacts with $[AuCl\{P(C_6H_4F\text{-}p)_3\}]$ to give $[Pt_3Au(\mu\text{-}SO_2)_3\{P(C_6H_{11})_3\}_3\{P(C_6H_4F\text{-}p)_3\}]PF_6$ which may be converted into (**2**) with NMe_4Cl. The compound $[Pt_3Au(\mu\text{-}SO_2)_3\{P(C_6H_{11})_3\}_3\{P(C_6H_4F\text{-}p)_3\}]PF_6$ and its chloride-bridged derivative (**2**) represent the first examples of compounds formed where $[Au(PR_3)]^+$ and $[AuCl(PR_3)]$ have been added to the same cluster compound. These studies indicate the occurrence of 54- and 56-electron tetrahedral Pt_3Au clusters analogous to the 42- and 44-electron triangular parent clusters.

Although much effort has been expended in the synthesis of platinum and gold cluster compounds,[1,2] relatively few examples of compounds with platinum–gold bonds are known. We recently reported the synthesis and structural characterisation of the first examples of platinum–gold clusters with tetrahedral, $[Pt_3Au(\mu\text{-}CO)_3\{P(C_6H_{11})_3\}_4]PF_6$,[3] and butterfly, $[Au_2Pt_2(PPh_3)_4(CNC_6H_3Me_2\text{-}2,6)_4][PF_6]_2$ geometries.[4] Braunstein *et al.*[5] have synthesised the triangular cluster compound $[Cl(Et_3P)_2PtAu_2(PPh_3)_2][CF_3SO_3]$ from *trans*-$[Pt(PEt_3)_2H(Cl)]$ and $[Au(thf)(PPh_3)_2][CF_3SO_3]$ (thf = tetrahydrofuran).

The compound $[Pt_3Au(\mu\text{-}CO)_3\{P(C_6H_{11})_3\}_4]PF_6$ was synthesised from $[Pt_3(\mu\text{-}CO)_3\{P(C_6H_{11})_3\}_3]$ and $[AuCl\{P(C_6H_{11})_3\}]$ in benzene solution in the presence of $TlPF_6$. An *X*-ray structural analysis confirmed the stoicheiometry and that the 54-electron cluster had resulted from capping of the $[Pt_3(\mu\text{-}CO)_3\{P(C_6H_{11})_3\}_3]$ triangle by a $[Au\{P(C_6H_{11})_3\}]^+$ fragment. The relatively low quality of the crystallographic data prevented an accurate structural determination. In this paper we report the synthesis and structural characterisation of the sulphur dioxide derivative of this compound and the synthesis of a platinum–gold 56-electron tetrahedral cluster compound.

Results and Discussion

The reaction of gaseous SO_2 at room temperature with $[Pt_3Au(\mu\text{-}CO)_3\{P(C_6H_{11})_3\}_4]PF_6$ in CH_2Cl_2 solution led to the substitution of one of the basal CO ligands and gave the compound $[Pt_3Au(\mu\text{-}CO)_2(\mu\text{-}SO_2)\{P(C_6H_{11})_3\}_4]PF_6$ (**1**) in high yield (>80%). Even when the reaction temperature was raised to 60 °C no further substitution resulted. The reaction of $[Pt_3(\mu\text{-}SO_2)_3\{P(C_6H_{11})_3\}_3]$ with $[AuCl(PR'_3)]$ in the absence of $TlPF_6$ in benzene solution at room temperature resulted in the formation of $[Pt_3Au(\mu\text{-}SO_2)_2(\mu\text{-}Cl)\{P(C_6H_{11})_3\}_3(PR'_3)]$ (**2**) in high yield (see Scheme). The most easily isolated and crystalline product was obtained when $PR'_3 = P(C_6H_4F\text{-}p)_3$. Compounds (**1**) and (**2**) were obtained as yellow and orange air-stable crystalline solids respectively. In solution the compounds are sensitive to oxygen and decompose over a period of hours.

In the presence of $TlPF_6$ in thf solvent at room temperature $[Pt_3(\mu\text{-}SO_2)_3\{P(C_6H_{11})_3\}_3]$ reacts with $[AuCl(PR_3)]$ to give $[Pt_3Au(\mu\text{-}SO_2)_3\{P(C_6H_{11})_3\}_3(PR_3)]PF_6$ $[PR_3 = P(C_6H_{11})_3$ or $P(C_6H_4F\text{-}p)_3]$ in high yield. The salt $[Pt_3Au(\mu\text{-}SO_2)_3\{P(C_6H_{11})_3\}_4]PF_6$ may be converted into (**1**) in good yield by reaction with gaseous CO at 50 °C in thf solution; $[Pt_3Au(\mu\text{-}SO_2)_3\{P(C_6H_{11})_3\}_3\{P(C_6H_4F\text{-}p)_3\}]PF_6$ may be converted into (**2**) in good yield by reaction with NMe_4Cl in benzene–ethanol solution at room temperature. These reactions are summarised in the Scheme. Their unusual feature is the addition of both $[Au(PR_3)]^+$ and $[AuCl(PR_3)]$ to the same cluster because the addition of the latter results in an increase in the cluster electron count of 2.

The i.r. spectrum of compound (**1**) as a Nujol mull shows the presence of bridging carbonyl (1 890, 1 832, and 1 804 cm^{-1}) and bridging sulphur dioxide[6] (1 233 and 1 075 cm^{-1}) ligands. The $^{31}P\text{-}\{^1H\}$ n.m.r. spectrum shows three resonances centred at 50.6, 60.7, and 82.0 p.p.m. with respect to trimethyl phosphate in the ratio 2:1:1 [see Figure 1(*a*)]. The resonances with smaller chemical shifts have splittings which can be associated with ^1J(P–Pt) couplings and are assigned to the phosphorus atoms attached to the Pt_3 triangle. The resonance at 82.0

† *Supplementary data available* (No. SUP 56341, 19 pp.): thermal parameters, complete bond lengths and angles. See Instructions for Authors, *J. Chem. Soc., Dalton Trans.*, 1986, Issue 1, pp. xvii—xx. Structure factors are available from the editorial office.

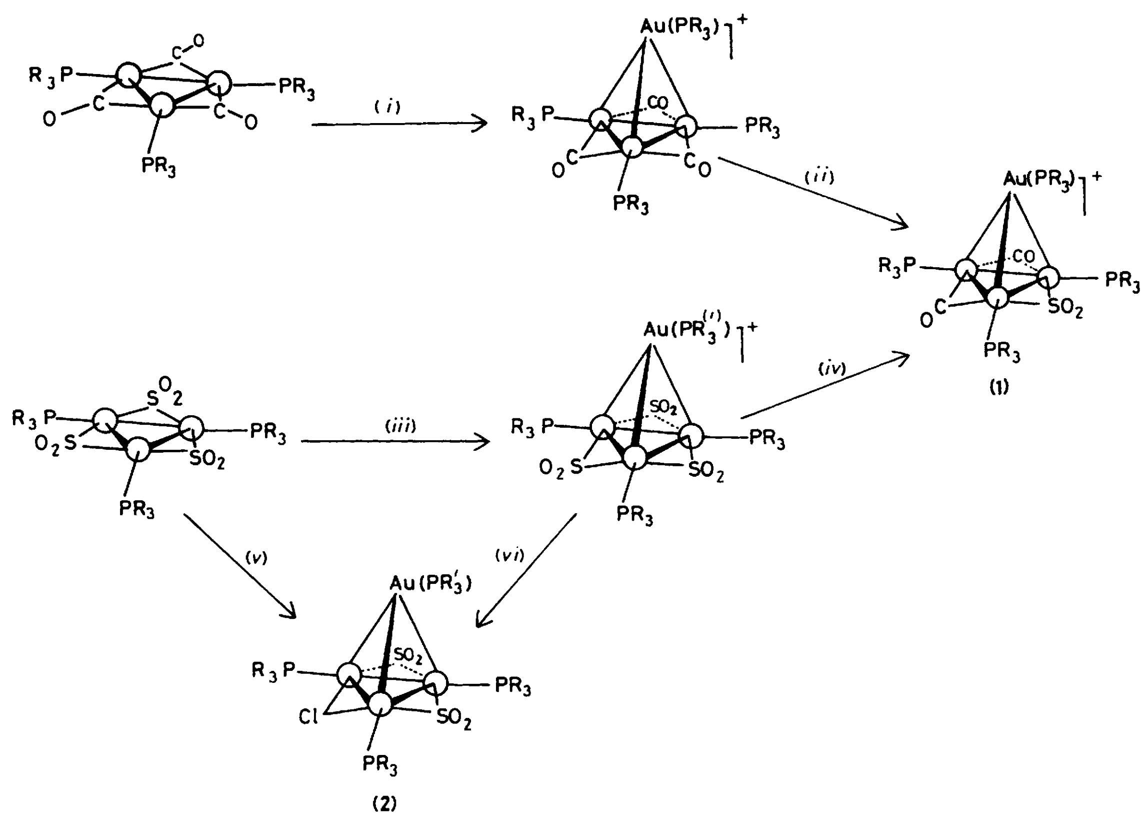

Scheme. ○, Pt; PR_3 = $P(C_6H_{11})_3$ and PR'_3 = $P(C_6H_4F\text{-}p)_3$. (*i*) $[Au(PR_3)]^+$, C_6H_6; (*ii*) SO_2, CH_2Cl_2; (*iii*) $[Au(PR_3)]^+$, thf; or $[Au(PR'_3)]^+$; (*iv*) CO, thf, 50 °C; (*v*) $[AuCl(PR'_3)]$, C_6H_6; (*vi*) NMe_4Cl, C_6H_6–EtOH

p.p.m. arises from the phosphorus atom attached to the capping gold atom. The spectrum has been satisfactorily simulated using a computer analysis based on a system comprised of the isotopomers A_2BC (no ^{195}Pt nuclei), AA'BCX (one ^{195}Pt nucleus, X), A_2BCY (one ^{195}Pt nucleus, Y), AA'BCXY (two ^{195}Pt nuclei, X and Y), AA'BCXX' (two ^{195}Pt nuclei, X and X'), and AA'BCXX'Y (three ^{195}Pt nuclei, X, X', and Y). The ^{195}Pt-$\{^1H\}$ n.m.r. spectrum shows two resonances at −4 636 p.p.m. [^1J(Pt–P) = 4 436 Hz] and −4 372 p.p.m. [^1J(Pt–P) = 4 705 Hz][7] with respect to $Na_2[PtCl_6]$ in the ratio 2:1, arising from the two different platinum sites in the molecule [see Figure 1(*b*)]. This was also analysed in terms of the spin system described above and is consistent with the molecule having C_s symmetry. The coupling constants derived from the computer simulations of the ^{31}P-$\{^1H\}$ and ^{195}Pt-$\{^1H\}$ spectra are given in Table 1.

The i.r. spectrum of compound **(2)** as a Nujol mull shows the presence of bridging sulphur dioxide ligands (1 185 and 1 052 cm^{-1}), and its ^{31}P-$\{^1H\}$ n.m.r. spectrum is similar to that of **(1)** having three resonances centred at 7.0, 16.8, and 29.5 p.p.m. with respect to trimethyl phosphate in the ratio 1:1:2. The ^{195}Pt-$\{^1H\}$ n.m.r. spectrum shows two resonances at −5 301 p.p.m. [^1J(Pt–P) = 4 800 Hz] and −4 049 p.p.m. [^1J(Pt–P) = 5 450 Hz] with respect to $Na_2[PtCl_6]$ in the ratio 1:2. Both spectra were analysed in terms of the spin system described for complex **(1)** and the coupling constants derived from the computer analysis are given in Table 2.

The i.r. spectrum of $[Pt_3Au(\mu\text{-}SO_2)_3\{P(C_6H_{11})_3\}_4]PF_6$ as a Nujol mull shows the presence of bridging sulphur dioxide ligands (1 264 and 1 087 cm^{-1}), and its ^{31}P-$\{^1H\}$ n.m.r. spectrum is similar to that reported for $[Pt_3Au(\mu\text{-}CO)_3\{P(C_6H_{11})_3\}_4]PF_6$ having two resonances centred at 60.3 and 83.1 p.p.m. with respect to trimethyl phosphate in the ratio 3:1. These resonances were assigned to the phosphorus atoms attached to the platinum triangle and the phosphorus atom attached to the capping gold atom respectively. The ^{195}Pt-$\{^1H\}$ n.m.r. spectrum shows a single resonance centred at −4 415 p.p.m. [^1J(Pt–P) = 4 117 Hz] with respect to $Na_2[PtCl_6]$. Both spectra were satisfactorily simulated using an analysis based on a system comprised of the isotopomers A_3B (no ^{195}Pt nuclei), $A_2A'BX$ (one ^{195}Pt nucleus, X) and AA'A''BXX' (two ^{195}Pt nuclei, X and X') and are consistent with the molecule having C_{3v} symmetry. The i.r. spectrum of $[Pt_3Au(\mu\text{-}SO_2)_3\{P(C_6H_{11})_3\}_3\{P(C_6H_4F\text{-}p)_3\}]PF_6$ as a Nujol mull shows the presence of bridging sulphur dioxide ligands (1 250 and 1 081 cm^{-1}). I.r. and ^{31}P-$\{^1H\}$ spectroscopy and analytical data were used to identify the products of the reactions of $[Pt_3Au(\mu\text{-}SO_2)_3\{P(C_6H_{11})_3\}_4]PF_6$ with CO and $[Pt_3Au(\mu\text{-}SO_2)_3\{P(C_6H_{11})_3\}_3\{P(C_6H_4F\text{-}p)_3\}]PF_6$ with NMe_4Cl.

The synthetic studies described above and summarised in the Scheme suggested the formation of 54- and 56-electron Pt_3Au clusters both with tetrahedral skeletal geometries. This is rather unusual since generally the addition of an electron pair to a cluster results in a skeletal rearrangement from tetrahedral to butterfly.[8] In order to confirm the structures of the clusters single-crystal *X*-ray crystallographic analyses on compounds **(1)** and **(2)** were undertaken. The relevant details are given in the Experimental section. Selected intramolecular bond lengths and angles for both molecules are given in Tables 3 and 4, fractional co-ordinates of the non-hydrogen atoms in Tables 5 and 6, and the structures are illustrated in Figures 2 and 3.

The four metal atoms in $[Pt_3Au(\mu\text{-}CO)_3\{P(C_6H_{11})_3\}_4]PF_6$, **(1)**, and **(2)** define slightly distorted tetrahedra with the Pt–Pt–Au, Pt–Pt–Pt, and Pt–Au–Pt angles close to the idealised angle of 60 °. In all three compounds the bridging ligands are attached exclusively to the platinum atoms and their

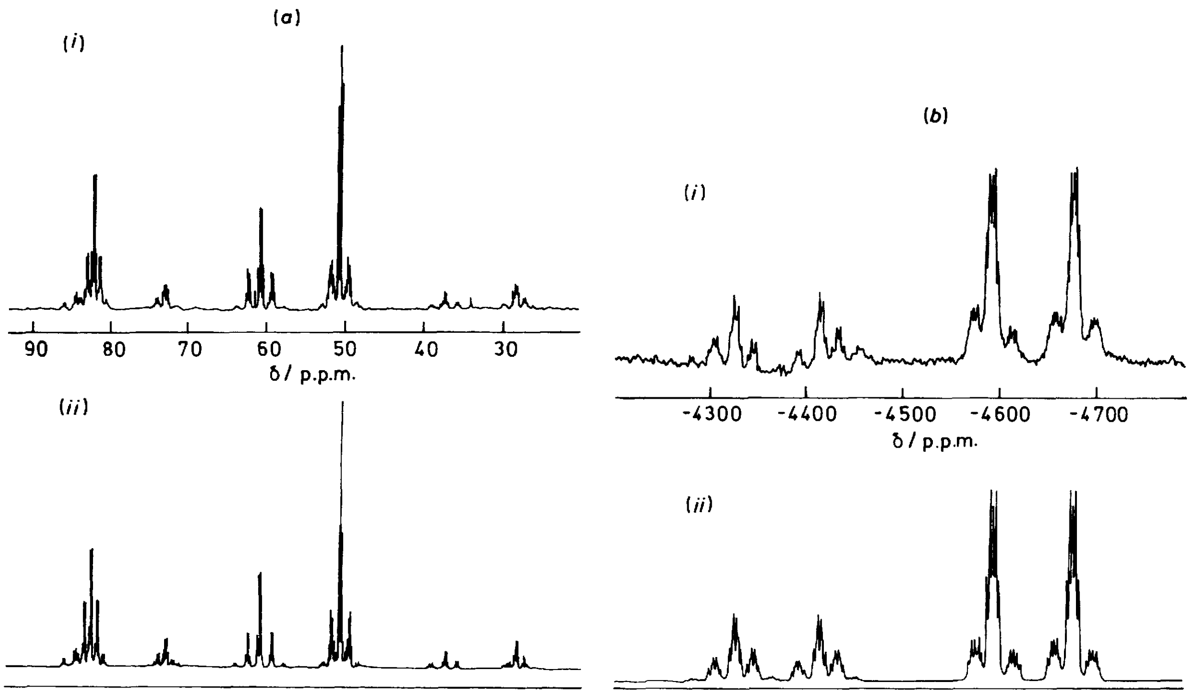

Figure 1. (*a*) observed (*i*) and calculated (*ii*) $^{31}P-\{^1H\}$ spectra for $[Pt_3Au(\mu-CO)_2(\mu-SO_2)\{P(C_6H_{11})_3\}_4]PF_6$, (**1**); (*b*) the corresponding $^{195}Pt-\{^1H\}$ spectra

Table 1. Chemical shifts and coupling constants for $[Pt_3Au(\mu-CO)_2(\mu-SO_2)\{P(C_6H_{11})_3\}_4]PF_6$, (**1**). Au(1) caps the Pt_3 triangle and is bonded to P(3) but is omitted for reasons of clarity in the schematic diagram below

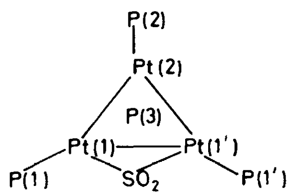

	P(1)	P(2)	P(3)	Pt(1)	Pt(2)
δ/p.p.m.	50.6	60.7	82.0	−4 636	−4 372

J/Hz

	Pt(1')	Pt(1)	Pt(2)	P(3)	P(2)	P(1)
P(1')	4 436	180	248	20	20	28
P(1)	180	4 436	248	20	20	
P(2)	308	308	4 705	20		
P(3)	166	166	166			
Pt(2)	2 167	2 167				
Pt(1)	*					

* It did not prove possible to estimate the value of ^1J[Pt(1)–Pt(1')] for this molecule since the resonances from the less-abundant isotopomers could not be distinguished from the overall spectra.

Table 2. Chemical shifts and coupling constants for $[Pt_3Au(\mu-SO_2)_2(\mu-Cl)\{P(C_6H_{11})_3\}_3\{P(C_6H_4F-p)_3\}]$, (**2**). Details as in Table 1

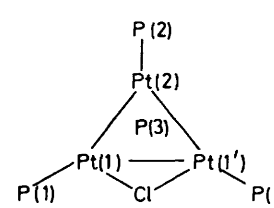

	P(1)	P(2)	P(3)	Pt(1)	Pt(2)
δ/p.p.m.	29.5	16.8	7.0	−4 049	−5 301

J/Hz

	Pt(1')	Pt(1)	Pt(2)	P(3)	P(2)	P(1)
P(1')	5 450	197	197	20	37	25
P(1)	197	5 450	197	20	37	
P(2)	220	220	4 800	20		
P(3)	250	250	250			
Pt(2)	1 468	1 468				
Pt(1)	*					

* It was not possible to estimate the value of ^1J[Pt(1)–Pt(1')] (see Table 1).

structures can be viewed in terms of a $[Au(PR_3)]^+$ fragment capping a $[Pt_3(\mu-X)_3\{P(C_6H_{11})_3\}_3]$ triangle. The bridging ligand atoms are essentially coplanar with the Pt_3 triangle and the phosphorus atoms are only displaced a small distance below this plane. In compound (**1**) they make an average angle of 15.8(6)° and in (**2**) 8.9(8)° with respect to the plane through the platinum atoms. Related capped structures have been observed in $[\{Pt_3(\mu-CNC_6H_3Me_2-2,6)_3(CNC_6H_3Me_2-2,6)_3\}_2Hg]$[9] and $[\{Pt_3(\mu-CO)_3(PPr^i_2Ph)_3Hg\}_2]$[10] although in the latter the deviations from planarity of the bridging ligands are greater. The Pt–Au distances within one molecule are not significantly different and essentially equal in (**1**) [2.757(1) Å] and (**2**) [2.769(1) Å] and comparable to that reported for $[Pt_3Au(\mu-CO)_3\{P(C_6H_{11})_3\}_4]PF_6$ [2.758(5) Å].[3] The Pt–Pt distances in

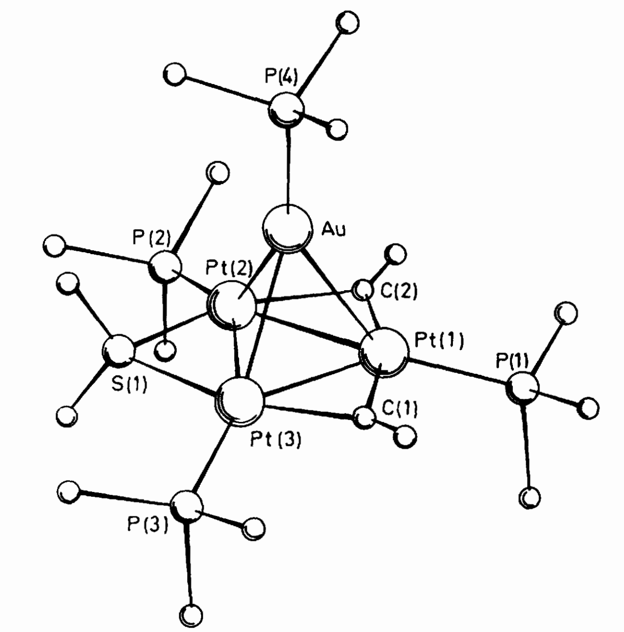

Figure 2. Illustration of the inner co-ordination sphere of $[Pt_3Au(\mu\text{-}CO)_2(\mu\text{-}SO_2)\{P(C_6H_{11})_3\}_4]PF_6$, **(1)**

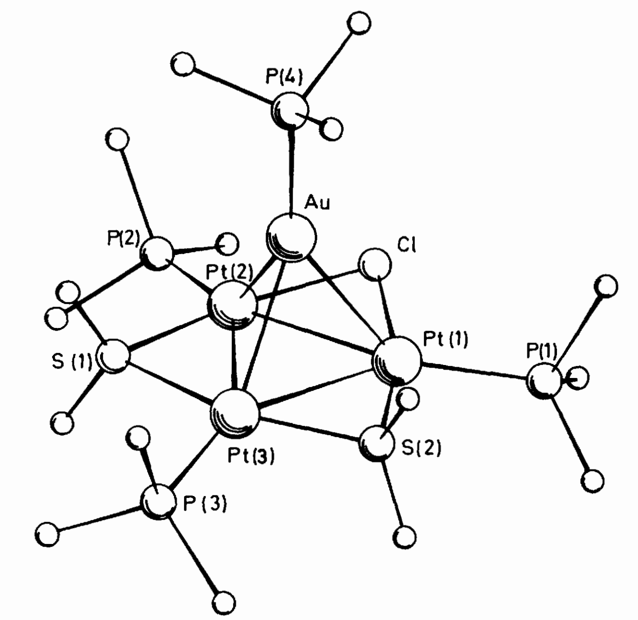

Figure 3. Illustration of the inner co-ordination sphere of $[Pt_3Au(\mu\text{-}SO_2)_2(\mu\text{-}Cl)\{P(C_6H_{11})_3\}_3\{P(C_6H_4F\text{-}p)_3\}]$, **(2)**

compound (**1**), 2.680(4), 2.667(4), and 2.746(1) Å, are similar to those reported for $[Pt_3Au(\mu\text{-}CO)_3\{P(C_6H_{11})_3\}_4]PF_6$ [average 2.696(9) Å] but shorter than those in (**2**), 2.869(1), 2.872(1), and 2.851(1) Å. This difference is not surprising in view of the fact that (**1**) has 54 valence electrons, making it isoelectronic with $[Au_4I_2(PPh_3)_4]$,[11] whereas (**2**) has 56 valence electrons, making it isoelectronic with $[Pt_4H_8(PPr^i{}_2Ph)_4]$;[12] $[Au_4I_2(PPh_3)_4]$ and $[Pt_4H_8(PPr^i{}_2Ph)_4]$ also have tetrahedral skeletal geometries.

Palladium and platinum show an interesting tendency to form both 42- and 44-electron triangular clusters. The former include $[Pt_3(\mu\text{-}CNBu^t)_3(CNBu^t)_3]$,[13] $[Pt_3(\mu\text{-}Ph)(\mu\text{-}PPh_2)(\mu\text{-}SO_2)(PPh_3)_3]$,[14] $[Pt_3(\mu\text{-}PPh_2)_2(\mu\text{-}H)(PPh_3)_3]^+$,[15] $[Pt_3(\mu\text{-}SO_2)_3(PPh_3)_3]$,[16] and $[Pt_3H_3(\mu\text{-}H)_3(PBu^t{}_3)_3]$.[12] In each case the platinum triangle is approximately equilateral and the Pt–Pt distances lie in the range 2.63—2.82 Å. The 44-electron clusters $[Pd_3(PPh_2)_2X(PR_3)_3]$[17] (X = Cl, Br, or SCF_3; R = Ph or Et) also have an approximately equilateral triangle of metal atoms but with longer metal–metal bonds (average Pd–Pd 2.92 Å for X = Cl and R = Et). Approximately equilateral 44-electron triangular clusters have been observed also in $[Pt_3(\mu\text{-}CO)_3\{P(C_6H_{11})_3\}_4]$[18] [average Pt–Pt 2.71(2) Å] and $[Pt_3(\mu\text{-}SO_2)_3\{P(C_6H_{11})_3\}_2\{Ph_2P(CH_2)_3PPh_2\}]$[19] [average Pt–Pt 2.80(2) Å]. Similarly, reduction of the 43-electron cluster $[Pt_3(CO)_3\{\mu\text{-}Fe(CO)_4\}_3]^-$ (average Pt–Pt 2.66 Å) to $[Pt_3(CO)_3\{\mu\text{-}Fe(CO)_4\}_3]^{2-}$ leads to a lengthening of all Pt–Pt

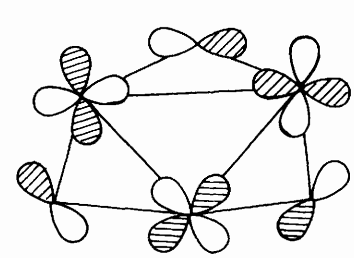

a_2'

bonds (average 2.75 Å).[20] In the tetrahedral platinum–gold cluster compounds described in this paper the $[Au(PR_3)]^+$ fragment has been shown to be capable of capping either 42- or 44-electron *triangulo*-clusters leading to electron counts of 54 and 56 respectively. In the trinuclear and tetranuclear complexes the additional electron pair resides in an orbital of a_2' symmetry which is localised primarily on the platinum triangle[21] (see below). Since this orbital is platinum–platinum antibonding its occupation leads to the observed lengthening of the Pt–Pt bond lengths in compound (**2**).

Experimental

Reactions were routinely carried out, using standard Schlenk-line procedures, under an atmosphere of pure, dry N_2 and using dry dioxygen-free solvents. Microanalyses (Cl, C, and H) were carried out by Mr. M. Gascoyne and his staff of this laboratory. Grating i.r. spectra were recorded for Nujol mulls using a Pye-Unicam SP2000 spectrometer and Fourier-transform i.r. spectra were recorded for Nujol mulls using a Perkin-Elmer 1 710 spectrometer.

Proton-decoupled ^{31}P and ^{195}Pt n.m.r. spectra were recorded using a Bruker AM-250 spectrometer. Samples for $^{31}P\text{-}\{^1H\}$ were referenced to $P(OMe)_3O$ in D_2O and for $^{195}Pt\text{-}\{^1H\}$ to $Na_2[PtCl_6]$ in D_2O. The machine operating frequencies were 101.26 MHz for ^{31}P and 53.55 MHz for ^{195}Pt. All samples were run in deuteriated solvents. N.m.r computer simulations were carried out using the Oxford University VAX computer system using a program developed by Professor R. K. Harris of the University of East Anglia and adapted for use at Oxford by Dr. A. E. Derome. The compound $[Pt_3(\mu\text{-}CO)_3\{P(C_6H_{11})_3\}_3]\cdot C_6H_6$ was synthesised by the method of Clark *et al.*[22] from *trans*-$[PtH_2\{P(C_6H_{11})_3\}_2]$ and CO, and $[Pt_3(\mu\text{-}SO_2)_3\{P(C_6H_{11})_3\}_3]$ was synthesised from $[Pt_3(\mu\text{-}CO)_3\{P(C_6H_{11})_3\}_3]\cdot C_6H_6$ and SO_2 by a method reported previously.[23]

Syntheses.—$[Pt_3Au(\mu\text{-}CO)_3\{P(C_6H_{11})_3\}_4]PF_6$. The compound $[Pt_3(\mu\text{-}CO)_3\{P(C_6H_{11})_3\}_3]\cdot C_6H_6$ (0.32 g, 0.2 mmol) was dissolved in benzene (20 cm^3) and $[AuCl\{P(C_6H_{11})_3\}]$

Table 3. Selected molecular dimensions (distances in Å, angles in °) for $[Pt_3Au(\mu\text{-}CO)_2(\mu\text{-}SO_2)\{P(C_6H_{11})_3\}_4]PF_6$ with estimated standard deviations in parentheses

Pt(1)–Pt(2)	2.680(4)	Pt(1)–Au–Pt(2)	58.2(1)
Pt(1)–Pt(3)	2.667(4)	Pt(1)–Au–Pt(3)	57.9(1)
Pt(2)–Pt(3)	2.746(1)	Pt(2)–Au–Pt(3)	59.70(4)
Pt(1)–Au	2.755(1)		
Pt(2)–Au	2.758(5)	Pt(2)–Pt(1)–Pt(3)	61.81(4)
Pt(3)–Au	2.759(5)	Pt(3)–Pt(1)–Au	61.2(1)
		Pt(2)–Pt(1)–Au	61.0(1)
Pt(1)–P(1)	2.294(6)		
Pt(2)–P(2)	2.31(2)	Pt(1)–Pt(2)–Pt(3)	58.9(2)
Pt(3)–P(3)	2.27(2)	Pt(1)–Pt(2)–Au	60.89(9)
Au–P(4)	2.243(7)	Pt(3)–Pt(2)–Au	60.2(2)
Pt(1)–C(1)	2.23(4)	Pt(1)–Pt(3)–Pt(2)	59.3(2)
Pt(3)–C(1)	2.07(4)	Pt(1)–Pt(3)–Au	61.0(1)
Pt(1)–C(2)	1.93(5)	Pt(2)–Pt(3)–Au	60.1(2)
Pt(2)–C(2)	2.12(5)		
Pt(2)–S	2.261(9)	C(1)–Pt(1)–C(2)	162(1)
Pt(3)–S	2.337(8)	P(1)–Pt(1)–C(1)	102(1)
		P(1)–Pt(1)–C(2)	97(1)
C(1)–O(1)	1.08(4)		
C(2)–O(2)	1.16(5)	S–Pt(2)–C(2)	159(1)
S–O(10)	1.50(2)	P(2)–Pt(2)–S	100(1)
S–O(20)	1.42(2)	P(2)–Pt(2)–C(2)	100(1)
Angles (°) between the plane Pt(1)–Pt(2)–Pt(3) and the bonds		S–Pt(3)–C(1)	164(1)
		P(3)–Pt(3)–S	102.2(5)
Pt(1)–P(1)	15.6	P(3)–Pt(3)–C(1)	94(1)
Pt(2)–P(2)	15.0		
Pt(3)–P(3)	16.9		

Table 4. Selected molecular dimensions (distances in Å, angles in °) for $[Pt_3Au(\mu\text{-}SO_2)_2(\mu\text{-}Cl)\{P(C_6H_{11})_3\}_3\{P(C_6H_4F\text{-}p)_3\}]$ with estimated standard deviations in parentheses

Pt(1)–Pt(2)	2.869(1)	Pt(1)–Au–Pt(2)	62.38(2)
Pt(1)–Pt(3)	2.872(1)	Pt(1)–Au–Pt(3)	62.50(2)
Pt(2)–Pt(3)	2.851(1)	Pt(2)–Au–Pt(3)	61.98(2)
Pt(1)–Au	2.769(1)		
Pt(2)–Au	2.771(1)	Pt(2)–Pt(1)–Pt(3)	59.55(2)
Pt(3)–Au	2.766(1)	Pt(3)–Pt(1)–Au	58.70(2)
		Pt(2)–Pt(1)–Au	58.83(2)
Pt(1)–P(1)	2.286(4)		
Pt(2)–P(2)	2.282(5)	Pt(1)–Pt(2)–Pt(3)	60.26(2)
Pt(3)–P(3)	2.288(4)	Pt(1)–Pt(2)–Au	58.78(2)
Au–P(4)	2.258(5)	Pt(3)–Pt(2)–Au	58.93(2)
Pt(2)–S(1)	2.270(5)	Pt(1)–Pt(3)–Pt(2)	60.18(2)
Pt(3)–S(1)	2.287(5)	Pt(1)–Pt(3)–Au	58.81(2)
Pt(1)–S(2)	2.304(5)	Pt(2)–Pt(3)–Au	59.09(2)
Pt(3)–S(2)	2.325(5)		
Pt(1)–Cl	2.353(5)	Cl–Pt(1)–S(2)	163.9(2)
Pt(2)–Cl	2.377(5)	P(1)–Pt(1)–Cl	96.7(2)
		P(1)–Pt(1)–S(2)	99.4(2)
S(1)–O(10)	1.41(2)		
S(1)–O(11)	1.45(2)	Cl–Pt(2)–S(1)	163.5(2)
S(2)–O(20)	1.34(2)	P(2)–Pt(2)–Cl	97.0(2)
S(2)–O(21)	1.42(2)	P(2)–Pt(2)–S(1)	99.4(2)
Angles (°) between the plane Pt(1)–Pt(2)–Pt(3) and the bonds		S(1)–Pt(3)–S(2)	162.5(2)
		P(3)–Pt(3)–S(1)	99.4(2)
Pt(1)–P(1)	10.0	P(3)–Pt(3)–S(2)	98.1(2)
Pt(2)–P(2)	9.4		
Pt(3)–P(3)	7.3		

(0.10 g, 0.2 mmol) and excess of $TlPF_6$ (0.21 g, 0.6 mmol) were added with stirring. After stirring for 1 h an orange solid was deposited and the supernatant solution became colourless. This solid was filtered off, dissolved in dichloromethane (30 cm^3), and filtered to remove excess of $TlPF_6$. On addition of benzene (20 cm^3) and removal of the dichloromethane *in vacuo*, orange crystals were obtained which were recrystallised from CH_2Cl_2–hexane by layering to yield the *product* (0.35 g, 81%) as small red crystals (Found: C, 42.7; H, 6.2. $C_{75}H_{132}AuF_6O_3P_5Pt_3$ requires C, 42.2; H, 6.2%); ν(CO) at 1 875vw, 1 805s, and 1 775vw cm^{-1} and $\nu(PF_6)$ at 843s cm^{-1}. The ^{31}P-{^1H} and ^{195}Pt-{^1H} n.m.r. spectra were reported previously.[3]

$[Pt_3Au(\mu\text{-}CO)_2(\mu\text{-}SO_2)\{P(C_6H_{11})_3\}_4]PF_6$, **(1)**. The compound $[Pt_3Au(\mu\text{-}CO)_3\{P(C_6H_{11})_3\}_4]PF_6$ (0.21 g, 0.1 mmol) was dissolved in dichloromethane (20 cm^3) and SO_2 gas was bubbled through the solution for 10 min. During this time the initially orange solution turned light yellow. On addition of benzene (30 cm^3) and removal of the dichloromethane *in vacuo* a yellow solid was obtained. This was recrystallised from dichloromethane–benzene by slow evaporation over a period of several days to yield the *product* (0.19 g, 86%) as yellow crystals (Found: C, 41.7; H, 6.1. $C_{74}H_{132}AuF_6O_4P_5Pt_3S$ requires C, 41.0; H, 6.1%); ν(CO) at 1 890m, 1 832s, and 1 804w cm^{-1}, $\nu(SO_2)$ at 1 233m and 1 075m cm^{-1}, and $\nu(PF_6)$ at 840s cm^{-1}.

$[Pt_3Au(\mu\text{-}SO_2)_2(\mu\text{-}Cl)\{P(C_6H_{11})_3\}_3\{P(C_6H_4F\text{-}p)_3\}]$, **(2)**. The compound $[Pt_3(\mu\text{-}SO_2)_3\{P(C_6H_{11})_3\}_3]$ (0.16 g, 0.1 mmol) was dissolved in benzene (20 cm^3) and $[AuCl\{P(C_6H_4F\text{-}p)_3\}]$ (0.054 g, 0.1 mmol) was added with stirring. Over a period of 10 min the red solution turned orange. The solvent was removed *in vacuo* giving a red oil which was recrystallised from dichloromethane–hexane to yield the *product* (0.17 g, 77%) as orange crystals. Crystals suitable for *X*-ray crystallography were grown by layering from benzene–hexane (Found: C, 45.2; H, 5.9; Cl, 1.7. $C_{72}H_{111}AuClF_3O_4P_4Pt_3S_2\cdot1.5C_6H_6$ requires C, 43.8; H, 5.4; Cl, 1.6%); $\nu(SO_2)$ at 1 185s and 1 052s cm^{-1}.

$[Pt_3Au(\mu\text{-}SO_2)_3\{P(C_6H_{11})_3\}_4]PF_6$. The compound $[AuCl\{P(C_6H_{11})_3\}]$ (0.10 g, 0.2 mmol) was dissolved in thf (30 cm^3) and excess of $TlPF_6$ (0.21 g, 0.6 mmol) was added with stirring. After 15 min this solution was filtered and added with stirring to a suspension of $[Pt_3(\mu\text{-}SO_2)_3\{P(C_6H_{11})_3\}_3]$ (0.32 g, 0.2 mmol) in thf (20 cm^3). The orange suspension slowly dissolved and after 0.5 h an orange solution was obtained. Ethanol (30 cm^3) was added to this solution and on removal of the thf *in vacuo* orange crystals of the *product* (0.35 g, 80%) were obtained (Found: C, 38.1; H, 6.5. $C_{72}H_{132}AuF_6O_6P_5Pt_3S_3$ requires C, 38.6; H, 5.9%); $\nu(SO_2)$ at 1 264m and 1 087s cm^{-1} and $\nu(PF_6)$ at 842s cm^{-1}. N.m.r.: ^{31}P-{^1H} (to high frequency of trimethyl phosphate), δ 60.3 [m, 3 P, $PtP(C_6H_{11})_3$, ^1J(Pt–P) 4 117, ^2J(Pt–P) 211, ^1J(Pt–Pt) 975, $^3J(P_{Pt}–P_{Pt})$ 29, $^3J(P_{Au}–P_{Pt})$ 15 Hz] and 83.1 p.p.m. [m, 1 P, $AuP(C_6H_{11})_3$, ^2J(Pt–P) 128, $^3J(P_{Au}–P_{Pt})$ 15 Hz]; ^{195}Pt-{^1H}, δ −4 415 p.p.m. (to low frequency of $Na_2[PtCl_6]$).

The compound $[Pt_3Au(\mu\text{-}SO_2)_3\{P(C_6H_{11})_3\}_3\{P(C_6H_4F\text{-}p)_3\}]PF_6$ was synthesised by a similar method to the $P(C_6H_{11})_3$ derivative described above (Found: C, 38.0; H, 5.4. $C_{72}H_{111}AuF_9O_6P_5Pt_3S_3$ requires C, 38.0; H, 4.9%); $\nu(SO_2)$ at 1 250m and 1 081s cm^{-1} and $\nu(PF_6)$ at 845s cm^{-1}.

Conversion of $[Pt_3Au(\mu\text{-}SO_2)_3\{P(C_6H_{11})_3\}_4]PF_6$ *into Compound* (1).—The compound $[Pt_3Au(\mu\text{-}SO_2)_3\{P(C_6H_{11})_3\}_4]PF_6$ (0.22 g, 0.1 mmol) was dissolved in thf (30 cm^3). This solution was heated to 50 °C and gaseous CO was bubbled through it for 15 min. During this period the initially orange solution turned light yellow and on addition of benzene (30 cm^3) and removal of the thf *in vacuo* a yellow crystalline solid

Table 5. Final fractional co-ordinates for non-hydrogen atoms of complex (1) with estimated standard deviations in parentheses

Atom	X/a	Y/b	Z/c	Atom	X/a	Y/b	Z/c
Pt(1)	0.315 56(5)	0.259 3(3)	0.092 19(3)	C(234)	0.250(2)	0.046(2)	0.252(1)
Pt(2)	0.192 7(2)	0.189 4(3)	0.099 6(1)	C(235)	0.239(2)	0.057(2)	0.199(1)
Pt(3)	0.193 7(2)	0.329 4(3)	0.099 7(1)	C(310)	0.198(2)	0.506(2)	0.102(1)
Au	0.221 56(5)	0.259 3(4)	0.016 79(4)	C(311)	0.199(2)	0.504(2)	0.047(1)
P(1)	0.436 4(3)	0.259 1(5)	0.106 8(2)	C(312)	0.249(2)	0.562(2)	0.028(1)
P(2)	0.144 3(8)	0.086 5(9)	0.123 7(6)	C(313)	0.226(2)	0.633(2)	0.046(1)
P(3)	0.148 3(8)	0.430 1(8)	0.126 1(6)	C(314)	0.223(2)	0.631(2)	0.102(1)
P(4)	0.207 5(4)	0.261(2)	−0.062 3(2)	C(315)	0.169(2)	0.576(2)	0.118(1)
S	0.094 9(4)	0.256 8(5)	0.105 7(3)	C(320)	0.048(2)	0.437(2)	0.119(1)
O(10)	0.046(1)	0.257 4(5)	0.063 8(7)	C(321)	0.025(1)	0.428(1)	0.066 4(8)
O(20)	0.059(1)	0.255 8(5)	0.150 5(7)	C(322)	−0.057(2)	0.417(2)	0.065(1)
C(1)	0.293(1)	0.370(2)	0.085(1)	C(323)	−0.093(2)	0.483(2)	0.083(1)
O(1)	0.325(1)	0.415(1)	0.075 5(8)	C(324)	−0.071(2)	0.496(2)	0.136(1)
C(2)	0.302(2)	0.162(2)	0.095(1)	C(325)	0.013(2)	0.504(2)	0.139(1)
O(2)	0.331(2)	0.110(2)	0.094(1)	C(330)	0.164(1)	0.442(1)	0.190 8(9)
C(110)	0.475(2)	0.175(2)	0.093(1)	C(331)	0.130(1)	0.380(1)	0.216(1)
C(111)	0.469(2)	0.168(2)	0.038(1)	C(332)	0.139(2)	0.385(2)	0.271(1)
C(112)	0.502(2)	0.098(2)	0.024(1)	C(333)	0.218(2)	0.385(2)	0.283(1)
C(113)	0.582(2)	0.092(2)	0.041(1)	C(334)	0.255(2)	0.444(2)	0.257(1)
C(114)	0.584(2)	0.100(2)	0.095(1)	C(335)	0.244(1)	0.440(2)	0.202(1)
C(115)	0.555(2)	0.171(2)	0.109(1)	C(410)	0.110(1)	0.256(2)	−0.076 1(9)
C(120)	0.454(1)	0.271(2)	0.172 0(7)	C(411)	0.078(2)	0.328(1)	−0.064(1)
C(121)	0.420(2)	0.335(2)	0.193(1)	C(412)	−0.003(2)	0.326(2)	−0.077(2)
C(122)	0.432(2)	0.339(1)	0.247(1)	C(413)	−0.041(2)	0.271(2)	−0.046(1)
C(123)	0.403(2)	0.275(2)	0.271 8(9)	C(414)	−0.009(2)	0.199(2)	−0.058(1)
C(124)	0.437(2)	0.210(2)	0.250(1)	C(415)	0.073(2)	0.200(2)	−0.045(1)
C(125)	0.423(3)	0.208(2)	0.196(1)	C(420)	0.240(2)	0.344(2)	−0.089(1)
C(130)	0.485(1)	0.336(1)	0.081 7(7)	C(421)	0.240(2)	0.349(2)	−0.143(1)
C(131)	0.470(2)	0.345(1)	0.028 1(8)	C(422)	0.257(2)	0.424(2)	−0.157(1)
C(132)	0.493(2)	0.418(2)	0.011(1)	C(423)	0.334(2)	0.439(2)	−0.142(1)
C(133)	0.573(2)	0.432(2)	0.023(1)	C(424)	0.343(2)	0.430(2)	−0.088(1)
C(134)	0.590(2)	0.418(2)	0.077(1)	C(425)	0.317(1)	0.360(1)	−0.071(1)
C(135)	0.566(1)	0.344(1)	0.090(1)	C(430)	0.255(2)	0.196(1)	−0.092(1)
C(210)	0.185(2)	0.016(2)	0.091(1)	C(431)	0.217(2)	0.169(2)	−0.136(1)
C(211)	0.181(2)	0.020(2)	0.037(1)	C(432)	0.268(3)	0.120(3)	−0.164(1)
C(212)	0.235(2)	−0.030(2)	0.016(1)	C(433)	0.281(3)	0.059(2)	−0.132(2)
C(213)	0.215(3)	−0.104(2)	0.030(1)	C(434)	0.319(3)	0.082(3)	−0.085(2)
C(214)	0.214(3)	−0.110(2)	0.084(1)	C(435)	0.274(3)	0.137(2)	−0.058(1)
C(215)	0.163(3)	−0.056(2)	0.107(2)	C(10)	0.449(4)	0.944(2)	0.182(2)
C(220)	0.050(2)	0.085(3)	0.117(2)	Cl(11)	0.415(2)	0.992(1)	0.136(1)
C(221)	0.028(2)	0.069(2)	0.064(1)	Cl(12)	0.460(3)	0.999(3)	0.230(1)
C(222)	−0.051(2)	0.089(2)	0.056(1)	C(20)	0.428(6)	0.494(4)	0.164(3)
C(223)	−0.100(2)	0.049(3)	0.092(2)	Cl(21)	0.423(3)	0.555(2)	0.119(2)
C(224)	−0.076(2)	0.058(2)	0.145(1)	Cl(22)	0.493(2)	0.515(2)	0.207(1)
C(225)	0.004(2)	0.040(2)	0.151(1)	C(30)	0.329(2)	0.258(3)	0.408(4)
C(230)	0.156(3)	0.063(3)	0.189(2)	Cl(31)	0.268(2)	0.190(2)	0.416(1)
C(231)	0.120(3)	0.120(3)	0.219(2)	Cl(32)	0.283(3)	0.328(2)	0.384(2)
C(232)	0.139(3)	0.112(3)	0.273(2)	P(5)	0.472(3)	0.750(4)	0.109(2)
C(233)	0.222(3)	0.108(2)	0.280(1)	P(6)	0.383(3)	0.765(5)	0.059(2)

(0.11 g, 52%) was obtained. This was identified as compound (**1**) by comparison of its i.r., $^{31}P-\{^1H\}$ n.m.r. spectroscopic and analytical data.

Conversion of $[Pt_3Au(\mu-SO_2)_3\{P(C_6H_{11})_3\}_3\{P(C_6H_4F-p)_3\}]PF_6$ *into Complex* (**2**).—$[Pt_3Au(\mu-SO_2)_3\{P(C_6H_{11})_3\}_3\{P(C_6H_4F-p)_3\}]PF_6$ (0.23 g, 0.1 mmol) was suspended in benzene–ethanol (10:1, 30 cm^3) and NMe_4Cl (0.033 g, 0.3 mmol) was added with stirring. After 10 min the initially red suspension changed to an orange solution. This was filtered and the solvent removed *in vacuo*. The orange residue was dissolved in dichloromethane (20 cm^3) and the solution filtered. On addition of methanol (30 cm^3) and removal of the dichloromethane under reduced pressure an orange crystalline solid (0.13 g, 58%) was obtained. This was identified as compound (**2**) by comparison of its i.r., $^{31}P-\{^1H\}$ n.m.r. spectroscopic and analytical data.

X-Ray Crystallography.—Crystal data for compound (**1**). $C_{74}H_{132}AuF_6O_4P_5Pt_3S\cdot CH_2Cl_2$, M = 2 253.7, orthorhombic, a = 18.671(4), b = 19.618(3), c = 28.162(4) Å, U = 10 315 Å^3 (by least-squares refinement on diffractometer angles for 25 automatically centred reflections, λ = 0.710 69 Å), space group $Pn2_1a$, Z = 4, D_c = 1.45 g cm^{-3}, $F(000)$ = 4 432. Large yellow crystals grown from dichloromethane–hexane by layering decomposed rapidly by loss of dichloromethane of crystallisation on removal from the mother-liquor, thus they were sealed surrounded by the mother-liquor in a 0.7-mm Lindemann capillary tube to avoid decomposition. Crystal dimensions 0.5 × 0.5 × 0.7 mm, $\mu(Mo\text{-}K_\alpha)$ = 59.2 cm^{-1}.

Geometric diffraction data were collected on a CAD4 diffractometer: ω—2θ scan with ω scan width 0.8°, graphite-monochromated Mo-K_α radiation; 7 076 reflections measured ($1 < \theta < 22°$), 3 501 unique absorption-corrected reflections with $I \geqslant 3\sigma(I)$, merging R = 0.0263.

Table 6. Final fractional co-ordinates for non-hydrogen atoms of complex (**2**) with estimated standard deviations in parentheses

Atom	*X/a*	*Y/b*	*Z/c*	Atom	*X/a*	*Y/b*	*Z/c*
Pt(1)	0.192 35(3)	0.093 80(3)	0.053 45(4)	C(234)	0.327 4(7)	0.342 9(8)	0.102(1)
Pt(2)	0.196 87(3)	0.201 35(2)	0.003 96(4)	C(235)	0.277 7(6)	0.318 4(7)	0.045(1)
Pt(3)	0.219 16(3)	0.124 85(3)	−0.133 92(4)	C(310)	0.204 3(6)	0.037 3(6)	−0.324(1)
Au	0.287 70(3)	0.141 71(3)	0.034 17(5)	C(311)	0.144 8(6)	0.032 8(7)	−0.326(1)
P(1)	0.162 7(2)	0.032 0(2)	0.151 9(3)	C(312)	0.128 6(8)	−0.024 6(7)	−0.329(1)
P(2)	0.174 0(2)	0.284 2(2)	0.037 3(3)	C(313)	0.146 5(7)	−0.050 5(8)	−0.421(1)
P(3)	0.230 5(2)	0.102 8(2)	−0.290 4(3)	C(314)	0.206 0(7)	−0.043 6(7)	−0.424(1)
P(4)	0.373 9(2)	0.141 8(2)	0.095 9(4)	C(315)	0.221 3(7)	0.014 4(7)	−0.418(1)
S(1)	0.219 6(2)	0.212 9(2)	−0.148 4(3)	C(320)	0.302 5(6)	0.099 0(6)	−0.303(1)
S(2)	0.213 6(2)	0.041 8(2)	−0.071 5(3)	C(321)	0.328 1(6)	0.056 2(6)	−0.236(1)
Cl	0.181 7(2)	0.164 7(2)	0.155 9(4)	C(322)	0.387 5(6)	0.053 0(7)	−0.244(1)
O(10)	0.269 6(7)	0.236 4(7)	−0.146(1)	C(323)	0.414 7(7)	0.105 1(7)	−0.224(1)
O(11)	0.177 1(7)	0.234 6(7)	−0.215(1)	C(324)	0.388 3(7)	0.146 4(8)	−0.292(2)
O(20)	0.260 1(8)	0.016 9(8)	−0.055(1)	C(325)	0.329 0(7)	0.151 7(6)	−0.281(1)
O(21)	0.170 1(8)	0.013 5(8)	−0.118(1)	C(330)	0.205 6(6)	0.152 3(7)	−0.383(1)
O(30)	0.128(1)	0.172(1)	0.174(2)	C(331)	0.145 4(7)	0.160 0(8)	−0.386(1)
O(31)	0.222(1)	0.169(1)	0.228(2)	C(332)	0.129 6(9)	0.209 2(8)	−0.445(1)
C(110)	0.119 4(6)	0.058 1(6)	0.238(1)	C(333)	0.145 7(8)	0.205 6(9)	−0.549(1)
C(111)	0.067 8(7)	0.080 9(7)	0.184(1)	C(334)	0.205 7(8)	0.195 6(8)	−0.541(2)
C(112)	0.037 2(8)	0.110 5(7)	0.257(1)	C(335)	0.219 5(7)	0.145 1(7)	−0.486(1)
C(113)	0.024 8(7)	0.074 1(8)	0.340(1)	C(410)	0.386 6(6)	0.168 1(4)	0.218(1)
C(114)	0.076 7(7)	0.051 5(8)	0.393(1)	C(411)	0.433 1(6)	0.194 1(4)	0.253(1)
C(115)	0.107 8(7)	0.021 7(6)	0.322(1)	C(412)	0.438 8(7)	0.214 9(5)	0.346(1)
C(120)	0.130 9(6)	−0.022 9(6)	0.082(1)	C(413)	0.396 9(7)	0.209 3(5)	0.401(1)
C(121)	0.084 4(7)	−0.006 2(6)	0.005(1)	C(414)	0.350 0(7)	0.183 6(5)	0.369(1)
C(122)	0.070 2(8)	−0.051 2(7)	−0.065(1)	C(415)	0.345 5(6)	0.162 7(5)	0.276(1)
C(123)	0.051 9(7)	−0.097 5(7)	−0.008(1)	C(420)	0.413 7(6)	0.180 4(5)	0.026 0(8)
C(124)	0.096 6(8)	−0.113 9(7)	0.072(1)	C(421)	0.389 3(6)	0.223 8(5)	−0.020 3(8)
C(125)	0.113 0(8)	−0.068 5(7)	0.141(1)	C(422)	0.419 4(7)	0.258 5(6)	−0.067 9(9)
C(130)	0.218 2(6)	0.002 0(6)	0.231(1)	C(423)	0.473 2(7)	0.249 0(6)	−0.068 3(9)
C(131)	0.246 7(6)	0.043 9(6)	0.297(1)	C(424)	0.498 5(6)	0.206 1(6)	−0.023 5(9)
C(132)	0.294 3(7)	0.021 1(7)	0.363(1)	C(425)	0.467 7(6)	0.171 7(6)	0.023 5(8)
C(133)	0.332 7(7)	−0.005 1(8)	0.301(1)	C(430)	0.403 5(6)	0.078 9(6)	0.098 7(9)
C(134)	0.304 0(7)	−0.047 8(7)	0.236(1)	C(431)	0.380 4(6)	0.042 2(6)	0.032 8(9)
C(135)	0.257 3(7)	−0.024 0(8)	0.169(1)	C(432)	0.402 8(7)	−0.007 0(6)	0.027(1)
C(210)	0.157 0(7)	0.325 5(6)	−0.070(1)	C(433)	0.449 0(7)	−0.017 0(7)	0.088(1)
C(211)	0.157 2(9)	0.384 1(7)	−0.053(1)	C(434)	0.472 9(6)	0.018 4(7)	0.155(1)
C(212)	0.151 3(9)	0.412 7(8)	−0.153(1)	C(435)	0.449 6(6)	0.067 0(7)	0.160(1)
C(213)	0.100 6(9)	0.395 0(8)	−0.216(2)	F(1)	0.405 4(8)	0.224 7(8)	0.497(1)
C(214)	0.101(1)	0.336 3(8)	−0.231(1)	F(2)	0.504 0(7)	0.280 9(7)	−0.115(1)
C(215)	0.104 7(8)	0.308 1(8)	−0.131(1)	F(3)	0.470 3(8)	−0.065 1(8)	0.084(1)
C(220)	0.122 0(6)	0.286 9(6)	0.120(1)	C(1)	0.019(2)	0.084(2)	−0.257(3)
C(221)	0.071 4(7)	0.257 3(8)	0.077(1)	C(2)	−0.007(2)	0.109(2)	−0.343(3)
C(222)	0.034 0(8)	0.251 9(8)	0.156(2)	C(3)	−0.005(2)	0.163(2)	−0.333(3)
C(223)	0.021 0(8)	0.305 7(8)	0.195(2)	C(4)	0.023(2)	0.184(2)	−0.254(3)
C(224)	0.070 8(8)	0.335 7(9)	0.235(1)	C(5)	0.052(2)	0.159(2)	−0.172(3)
C(225)	0.108 5(8)	0.340 8(7)	0.156(1)	C(6)	0.048(2)	0.111(2)	−0.185(3)
C(230)	0.231 7(6)	0.317 7(7)	0.106(1)	C(7)	0.477(3)	0.056(3)	0.501(7)
C(231)	0.248 0(7)	0.289 3(7)	0.204(1)	C(8)	0.512(4)	0.028(4)	0.559(7)
C(232)	0.296 8(7)	0.315 6(8)	0.262(1)	C(9)	0.527(4)	−0.020(4)	0.560(7)
C(233)	0.343 1(7)	0.315 1(8)	0.200(1)				

The structure was solved by direct methods (MULTAN) originally under the space group *Pnma* with Pt(1), Au, P(1), P(4), and S lying on a mirror plane and Pt(2) and Pt(3) symmetrically disposed on either side of it. In this space group the phosphine ligands were found to be highly disordered, thus the mirror plane was removed with consequent lowering of the space-group symmetry to $Pn2_1a$. This led to an ordered structure for the cationic moiety with Pt(1), Au, P(1), P(4), and S defining a pseudo-mirror plane with the different conformations of the tricyclohexyl groups breaking the mirror symmetry. Refinement was by blocked-matrix least-squares methods, Pt, Au, P, and S atoms anisotropic and the remainder isotropic. A Chebyshev weighting scheme with coefficients 575.9, 790.6, and 242.7 gave satisfactory agreement analyses. Final *R* and *R'* values were 0.0472 and 0.0692. The counter ion, PF_6^-, was not located with certainty. The remaining peaks in the penultimate difference Fourier map were assigned to phosphorus atoms having low occupancy and the final Fourier difference map revealed numerous peaks around these phosphorus sites which were associated with heavily disordered fluorine atoms. No completely satisfactory analysis of the disorder was possible because of the multitude of fluorine positions revealed. A Fourier-transform i.r. spectrum for the single crystal used for *X*-ray diffraction showed a strong peak at 840 cm^{-1} which was attributed to PF_6^-.

Crystal data for compound (**2**). $C_{72}H_{111}AuClF_3O_4P_4Pt_3S_2\cdot 1.5\ C_6H_6$, $M = 2\,220.3$, monoclinic, $a = 25.490(4)$, $b = 25.855(6)$, $c = 13.819(4)$ Å, $\beta = 96.98(2)°$, $U = 9\,040$ Å^3 (by least-squares refinement on diffractometer angles for 25 automatically centred reflections, $\lambda = 0.710\,69$ Å), space group $P2_1/n$,

$D_m = 1.69$ g cm^{-3}, $Z = 4$, $D_c = 1.63$ g cm^{-3}, $F(000) = 4\,348$. A red crystal grown from benzene–hexane was sealed in a 0.5-mm Lindemann capillary tube. Crystal dimensions 0.5 × 0.3 × 0.2 mm, λ(Mo-K_α) = 67.3 cm^{-1}.

Data were collected using the same scanning mode as above with ω scan width 0.9°; 15 424 reflections measured (1.5 < θ < 22.5°), 6 852 unique absorption-corrected reflections with $I \geqslant 3\sigma(I)$, merging $R = 0.0439$.

The structure was solved by standard Patterson and Fourier methods and refined as above. A Chebyshev weighting scheme with coefficients 163.3, 217.4, and 75.4 gave satisfactory agreement analyses. Final R and R' values were 0.0423 and 0.0582. The bridging SO_2 and Cl units were found to be disordered around the base of the tetrahedron and the occupancies of the oxygen atoms attached to the basal bridging atoms were refined. The results of this refinement suggested that suitable values for the occupancies of the attached oxygens were close to 0.75, 0.75, and 0.5. Thus their occupancies were set to these values and their isotropic thermal parameters were refined satisfactorily.

The crystallographic analyses were carried out on the Oxford University Chemical Crystallography VAX computer system. The programs used and the sources of scattering-factor data are given in ref. 24.

References

1 F. R. Hartley, 'Comprehensive Organometallic Chemistry,' eds. G. Wilkinson, F. G. A. Stone, and E. W. Abel, Pergamon Press, Oxford, 1982, vol. 6, p. 471.

2 K. P. Hall and D. M. P. Mingos, *Prog. Inorg. Chem.*, 1984, **32**, 237.

3 C. E. Briant, R. W. M. Wardle, and D. M. P. Mingos, *J. Organomet. Chem.*, 1984, **267**, C49.

4 C. E. Briant, D. I. Gilmour, and D. M. P. Mingos, *J. Organomet. Chem.*, 1984, **267**, C52.

5 P. Braunstein, H. Lehner, D. Matt, A. Tiripicchio, and M. Tiripicchio-Camellini, *Angew. Chem.*, 1984, **96**, 307.

6 D. M. P. Mingos, *Transition Met. Chem.*, 1978, **3**, 1; R. R. Ryan, G. J. Kubas, D. C. Moody, and P. G. Eller, *Struct. Bonding (Berlin)*, 1981, **46**, 47.

7 P. S. Pregosin, *Coord. Chem. Rev.*, 1982, **44**, 245.

8 D. M. P. Mingos, *Acc. Chem. Res.*, 1984, **17**, 311 and refs. therein.

9 Y. Yamamoto, H. Yamazaki, and T. Sakurai, *J. Am. Chem. Soc.*, 1982, **104**, 2329.

10 A. Albinati, A. Moor, P. S. Pregosin, and L. M. Venanzi, *J. Am. Chem. Soc.*, 1982, **104**, 7672.

11 F. Demartin, M. Manassero, L. Naldini, R. Ruggeri, and M. Sansoni, *J. Chem. Soc., Chem. Commun.*, 1981, 22.

12 P. W. Frost, J. A. K. Howard, J. L. Spencer, D. G. Turner, and D. Gregson, *J. Chem. Soc., Chem. Commun.*, 1981, 1104.

13 M. Green, J. A. K. Howard, M. Murray, J. L. Spencer, and F. G. A. Stone, *J. Chem. Soc., Dalton Trans.*, 1977, 1509.

14 D. G. Evans, G. R. Hughes, D. M. P. Mingos, J-M. Bassett, and A. J. Welch, *J. Chem. Soc., Chem. Commun.*, 1980, 1255.

15 P. L. Bellon, A. Ceriotti, F. Demartin, G. Longoni, and B. T. Heaton, *J. Chem. Soc., Dalton Trans.*, 1982, 1671.

16 D. C. Moody and R. R. Ryan, *Inorg. Chem.*, 1977, **16**, 1052.

17 G. W. Bushnell, K. R. Dixon, P. M. Moroney, A. D. Rattray, and C. Wan, *J. Chem. Soc., Chem. Commun.*, 1977, 709.

18 A. Albinati, G. Carturan, and A. Musco, *Inorg. Chim. Acta*, 1976, **16**, L3.

19 M. F. Hallam, N. D. Howells, D. M. P. Mingos, and R. W. M. Wardle, *J. Chem. Soc., Dalton Trans.*, 1985, 845.

20 G. Longoni, M. Manassero, and M. Sansoni, *J. Am. Chem. Soc.*, 1980, **102**, 7973.

21 D. G. Evans, G. R. Hughes, D. M. P. Mingos, J-M. Bassett, and A. J. Welch, *J. Chem. Soc., Chem. Commun.*, 1980, 1255; D. G. Evans and D. M. P. Mingos, *J. Organomet. Chem.*, 1982, **240**, 321; *ibid.*, 1983, **251**, C13; D. J. Underwood, R. Hoffmann, K. Tatsumi, A. Nakamura, and Y. Yamamoto, *J. Am. Chem. Soc.*, in the press; N. A. McEvoy, Part II Thesis, University of Oxford, 1980.

22 H. C. Clark, A. B. Goel, and C. S. Wong, *Inorg. Chim. Acta*, 1977, **34**, 159.

23 C. E. Briant, D. G. Evans, and D. M. P. Mingos, *J. Chem. Soc., Chem. Commun.*, 1982, 1144.

24 J. R. Carruthers, CRYSTALS User Manual, Oxford University Computing Centre, 1975; K. Davies, CHEMGRAF User Manual, Chemical Crystallography Laboratory, Oxford, 1981; 'International Tables for *X*-Ray Crystallography,' Kynoch Press, Birmingham, 1974, vol. 4, p. 99.

Received 26th March 1985; Paper 5/504